ACS EARTH AND SPACE CHEMISTRY

http://pubs.acs.org/journal/aesccq
Article

Complex Hygroscopic Behavior of Ambient Aerosol Particles Revealed by a Piezoelectric Technique

Christi Jose,* Aishwarya Singh, Kavyashree N. Kalkura, George V. Jose, Shailina Srivastava, Rameshchand K. Ammini, Shweta Yadav, Raghunathan Ravikrishna, Meinrat O. Andreae, Scot T. Martin, Pengfei Liu,* and Sachin S. Gunthe*

Cite This: ACS Earth Space Chem. 2024, 8, 983−991
Read Online

ABSTRACT: Understanding the complex interactions between atmospheric aerosols and water vapor in subsaturated regions of the atmosphere is crucial for modeling and predicting aerosol−cloud−radiation−climate interactions. However, the microphysical mechanisms of these interactions for ambient aerosols remain poorly understood. For this study, size-resolved samples were collected from a high-altitude, relatively clean site situated in the Western Ghats of India during the monsoon season, in order to study background and preindustrial processes as a baseline for climate functioning within the context of the most polluted region of the world. Measurements of humidity−dependent mass-based growth factors, hygroscopicity, deliquescence behavior, and aerosol liquid water content (ALWC) were made by a novel approach using a quartz crystal microbalance based on a piezo-electric sensor. The climate-relevant fine-mode aerosols (≤2.5 μm) exhibited strong size-dependent variations in their interactions with water vapor and contributed a high fraction of ALWC. Deliquescence occurred for relatively large aerosols (diameter >180 nm) but was absent for smaller aerosols. The deliquescence relative humidity for ambient aerosols was significantly lower than that of pure inorganic salts, suggesting a strong influence of organic species. Our study establishes an improved approach for accurately measuring aerosol water uptake characteristics of ambient aerosols in the subsaturated regime, aiding in the assessment of radiative forcing effects and improving climate models.

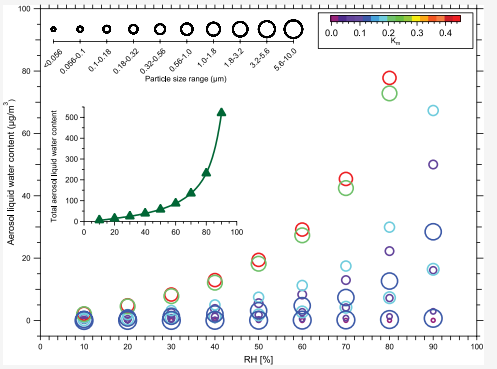

KEYWORDS: *radiation−climate interaction, tropical India, preindustrial conditions, biogenic SOA, size-resolved aerosol deliquescence, mass-based hygroscopicity, QCM*

1. INTRODUCTION

A comprehensive understanding of the hygroscopicity that determines the size, refractive indices, and cloud condensation nuclei properties of atmospheric particles is essential in assessing their impact on global climate and local visibility.[1] Investigation of the hygroscopicity of ambient aerosols poses significant challenges due to their chemical complexity, particle size variation, phase state, and viscosity.

Various techniques such as Fourier transform infrared spectroscopy (FTIR),[2,3] quartz crystal microbalance (QCM),[4−7] Raman spectroscopy,[8,9] electrodynamic balance (EDB),[10−12] optical microscopy (OM),[13−15] hygroscopicity tandem differential mobility analysis (HTDMA),[1,16,17] and size-selected cloud condensation nuclei (CCN) spectrometry[18−20] have been utilized to investigate the hygroscopicity of laboratory-generated as well as ambient aerosols.[21] However, no consensus exists on the most effective method for measuring the hygroscopicity, leading to inconsistent and incomparable results among studies. Most hygroscopicity measurements focus on particles in the accumulation mode, and measurements for nucleation and coarse mode particles, which exhibit complex hygroscopic behaviors, are limited. The large variations in the hygroscopic properties and composition of organic and inorganic species present in atmospheric aerosol particles result in a wide range of growth factors and phase transitions. Such behaviors need to be accurately determined to be considered in climate models.[22]

The QCM method has been effectively used to determine the mass-based hygroscopicity and physical property variations of laboratory-generated atmospherically relevant organic and inorganic aerosols.[4,23,24] This technique overcomes the limitations of other methods, such as the HTDMA, which is restricted to a narrow particle size range with limited relative humidity (RH) resolution.[25] The conventional HTDMA

Received: December 2, 2023
Revised: March 22, 2024
Accepted: March 28, 2024
Published: April 18, 2024

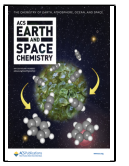

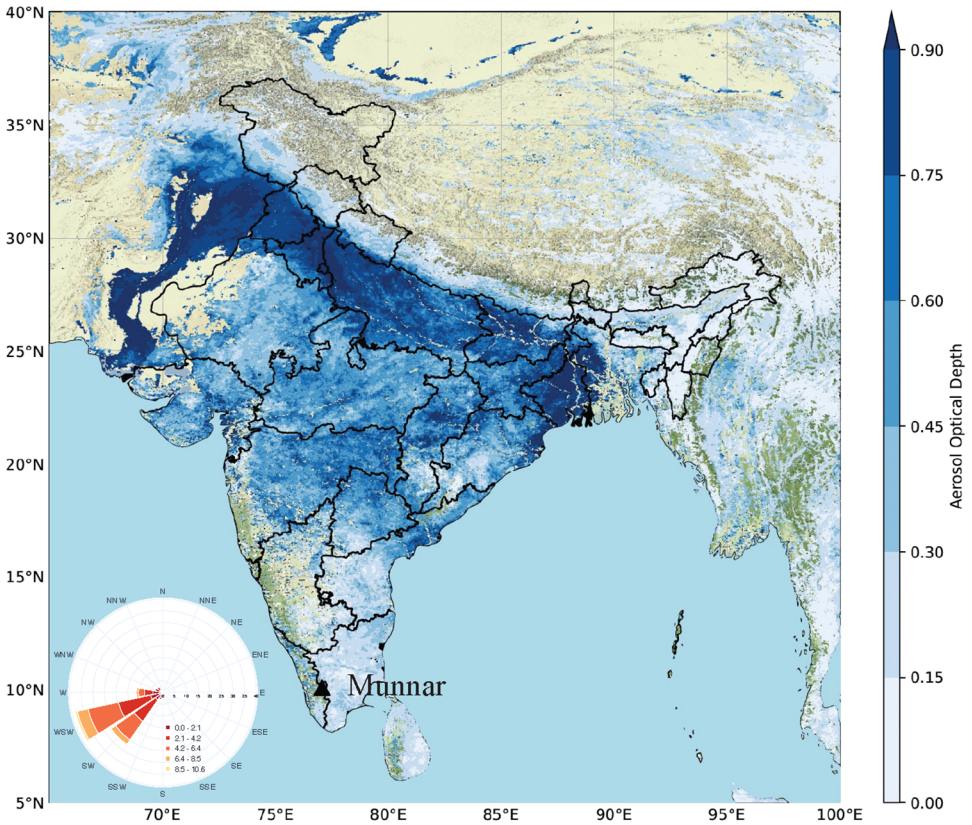

Figure 1. Spatial distribution of average aerosol optical depth (AOD) derived from MODIS (moderate resolution imaging spectroradiometer) level 2 data over the Indian continental region during the monsoon season of 2021 (June−September). The AOD distribution clearly indicates a relatively low aerosol loading over the observational site of Munnar (marked as a black triangle) compared with other parts of India. The wind rose diagram shown in the inset is the average wind speed and wind direction arriving at the sampling site during the ambient aerosol sampling period (August−September 2021). The prevailing air masses mostly originated over the Indian Ocean and arrived from the southwest directions, bringing clean marine influx to the observational site, confirming the relatively low influence of anthropogenic activities.

methods are inadequate in revealing the heterogeneity of hygroscopicity and phase transition within a wider aerosol size range, which substantially impacts atmospheric processes such as cloud condensation nuclei (CCN) activation and aerosol liquid water.[22] Mass-based measurements using QCM can accurately quantify the hygroscopic behavior of aerosol particles exposed to a wide range of RH in the atmosphere and the physical property variations during phase transitions. The wide RH range possible with measurements by QCM also helps to delineate mechanisms of water uptake, such as solubility and water diffusion limitations.[23,26]

India's climate is distinct and intricate, and according to the country's initial climate change assessment report of 2020, India has experienced significant challenges, such as temperature increase and extreme weather events since the mid-twentieth century. A significant challenge in addressing these issues is the lack of systematic measurements of aerosol characteristics, particularly regarding aerosol−water vapor interactions in the subsaturated regime, i.e., where the RH is below 100%.[1] Given that the sampling location represents a relatively pristine environment surrounded by forest in the Western Ghats of India, it is anticipated that aerosol particles collected from this region will contain a substantial fraction of organic material derived from biogenic precursors.[27] The dynamic chemical transformation of secondary organic aerosols (SOA) in the atmosphere results in a complex composition of biogenic SOA. Further atmospheric processing of complex SOA makes it difficult to understand the phase state and other properties of atmospheric aerosols.[28] In this study, we employ QCM measurements to obtain the dependence of aerosol hygroscopicity on RH, chemical composition, and size for a wide range of ambient aerosols from a relatively pristine location in India.

2. MATERIALS AND METHODS

Size-resolved ambient aerosols were sampled at the Natural Aerosol and Bioaerosol High Altitude (NABHA) Laboratory at the College of Engineering, Munnar (10.0930° N, 77.0682° E; 1600 m above mean sea level), a high-altitude and typically clean site situated in the Western Ghats of India. Munnar possesses a moderately rugged topography with high mountain peaks and deep river valleys covered with diverse vegetated areas, tea garden areas, forest, and water bodies constituting ∼70−75% of the land-use area.[27] Ambient particles were collected on PTFE (polytetrafluoroethylene) filters using a 10-stage micro-orifice uniform deposit impactor (MOUDI-II 120-R, TSI)[29,30] during the monsoon season (August−September) of 2021. The particles were subsequently transferred to a hydrophobic SiO_2-coated quartz sensor by gently pressing the filter paper onto the sensor. The hygroscopic growth factor, hygroscopicity parameter, and deliquescence relative humidity (DRH) were estimated using a highly sensitive mass balance instrument, QCM (QSense Analyzer, Biolin Scientific).[7,31] The accuracy and robustness of the method were demonstrated by performing measurements of the hygroscopic growth factor

https://doi.org/10.1021/acsearthspacechem.3c00347
ACS Earth Space Chem. 2024, 8, 983−991

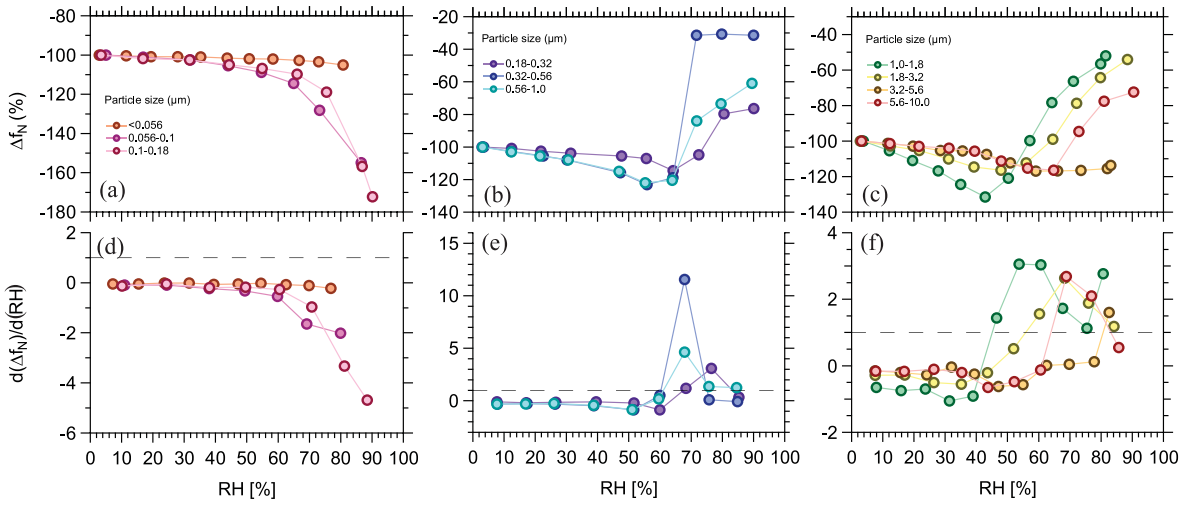

Figure 2. Deliquescence phase transition behavior of size-resolved ambient aerosol particles from Munnar. For panels (a−c), Δf_N represents the change in the oscillation frequency of the quartz crystal microbalance (QCM) sensor resulting from water uptake by the aerosol particles at different relative humidity (RH) conditions normalized to that of the dry aerosol particles at RH < 5%, expressed as percentage. The decrease in the value of Δf_N for each size range for the sampled ambient aerosol particles indicates the water uptake under different RH conditions in the subsaturated regime. The solid markers and lines identify different particle size ranges. In panels (d−f), the derivative of Δf_N with respect to RH ($d(\Delta f_N)/d(RH)$) is plotted against RH to determine the deliquescence relative humidity (DRH) value corresponding to the respective aerosol size ranges. The RH values at which $d(\Delta f_N)/d(RH)$ becomes ≥1 (marked by the dashed line) represent the DRH values for the individual aerosol size ranges.

and DRH for sucrose and $(NH_4)_2SO_4$ particles, respectively, which were compared with previously reported results[6,32−37] (Figures S3 and S4). The hygroscopic growth factor and the corresponding hygroscopicity parameter, κ, were determined over a wide range of RH conditions using κ-Köhler theory,[38] where κ represents a quantitative measure of aerosol water uptake characteristics.[39] The water uptake characteristics and the phase transition behaviors of the ambient samples were investigated and compared between different size ranges of particles below 10 μm collected using the MOUDI sampler. The aerosol liquid water content (ALWC)[40] at different RH conditions was also estimated from corresponding hygroscopicity parameters for each size range of particles. The number size distributions of the ambient aerosol particles of dry mobility diameter 10 to 420 nm [measured in parallel using a scanning mobility particle sizer, SMPS, composed of an electrostatic classifier (EC, TSI Model 3082) equipped with a differential mobility analyzer (DMA, TSI Model 3081) and a condensation particle counter (CPC, TSI Model 3750)] were then converted to mass size distributions assuming a particle density of 1.2 g cm^{-3}.[41] The supermicrometer particle mass size distribution for the same season, but a different year, was used in this study, which had been obtained using an ultraviolet aerodynamic particle sizer (UV-APS, TSI Inc., model 3314).[42]

Meteorological parameters were recorded by using an automatic weather station (AWS, Clima Sensor US) during the sampling period. Figure 1 shows the sampling site, Munnar, along with aerosol optical depth (AOD) over India during the monsoon season, indicating the relatively pristine nature of the sampling site. During the measurement, airmasses predominantly arrived from the southwest direction, bringing clean marine influx to the observational site and resulting in a low influence of anthropogenic emissions (Figure 1).

A more detailed description of the instruments, experimental techniques, and estimation of various parameters is provided in the Supporting Information (SI).

3. RESULTS AND DISCUSSION

The oscillation frequency variation (Δf) of the QCM sensor reflects the water uptake and release, and the frequency variation data can be interpreted to understand physical processes, such as adsorption, desorption, and those indicative of the physical state of aerosol particles on the sensor during the solid to aqueous phase transition.[43] Normalizing the frequency shift induced by the aerosol particles at a given RH to the frequency shift resulting from a deposited dry sample (RH < 5%) yields a percentage value denoted by Δf_N.[6] Figure 2 shows the corresponding Δf_N calculated for the ambient aerosol particles as a function of RH for different sampled size ranges. A negative sign in Δf_N indicates that the frequency decreases when RH increases due to water uptake. Text S6 provides more details about the estimation of Δf_N and the derivative of Δf_N as a function of RH, $d(\Delta f_N)/d(RH)$.

For the particle size ranges of <180 nm (Figure 2a), the Δf_N decreased, implying water uptake, with the particles <56 nm displaying the lowest value. In Figure 2b,c, the particles exhibit higher water uptake when compared to smaller particles (<180 nm; Figure 2a) under lower RH conditions, as indicated by the decrease in Δf_N. However, the Δf_N values suddenly increase at a certain RH, implying a drastic increase in the water uptake, which led to a phase transition caused by deliquescence. Figure 2d−f shows that particles above 180 nm display deliquescence at different RH values (known as the DRH), and those below 180 nm do not. Various studies in the past have reported the absence of deliquescence for ambient and laboratory-generated atmospherically relevant particles even at very high RH values and concluded the particles to be organic in nature.[6,35,36,44] Accordingly, we hypothesize that the particles in the size range <180 nm were probably dominated by freshly formed SOA resulting from the oxidation of biogenic volatile organic compounds (VOCs), given the densely vegetated/forest region and season. Concomitant quasi-continuous measurements conducted during the same campaign indicated as high as

https://doi.org/10.1021/acsearthspacechem.3c00347
ACS Earth Space Chem. 2024, 8, 983−991

~90% of organic fraction in NR-PM_1 (nonrefractory particulate matter with an aerodynamic diameter ≤1 μm; Table S2), and the details will be discussed in follow up studies.

As described by Chao et al.,[6] the RH corresponding to $d(\Delta f_N)/d(RH) \geq 1$ signifies the DRH of the given aerosol sample. For multicomponent externally mixed aerosol particles, multiple DRH values are expected. On the other hand, internally mixed aerosol particles would exhibit a single DRH value expected to be in between the DRH values of the individual components, as observed in the present study. Based on this criterion, we observed DRH in the range of ~60−68% for three size ranges (180−320 nm; 320−560 nm; 560 nm−1 μm) sampled in this study (Figure 2e). As the size range exceeded 180 nm, the presence of inorganic salts, like $(NH_4)_2SO_4$, might have contributed to the appearance of a DRH[45] (Figure 2b,e). Further, these DRH values were lower than that of pure $(NH_4)_2SO_4$ (DRH = 80%), potentially due to the presence of mixed salts and/or organic compounds in the sampled aerosol particles. The deliquescence behavior of organic−inorganic mixtures results in complexity due to the solubility limitations depending on the type of organic species present in the aerosol particles. The previous studies on the phase transition behavior of organic−inorganic mixtures have reported reduced DRH of the inorganic species, while in some cases the presence of organics did not affect the DRH of inorganic species.[46−48] Thus, we hypothesize that particles in the size range of 180 nm to 1 μm at this site predominantly reflected a complex mixture of inorganic salts such as $(NH_4)_2SO_4$ and water-soluble organic compounds. The supermicrometer aerosol particles (>1 μm), except the size range between 1 and 1.8 μm, exhibited a <17% change in Δf_N indicating relatively lower water uptake (Figure 2c). Beyond the maximum water uptake indicated by Δf_N, the three particle size ranges showed different DRH values. For example, 1.8−3.2 and 5.6−10 μm exhibited DRH between 56 and 68%, again indicating a complex mixture of water-soluble organic compounds and inorganic salts, whereas the particles for the size range 3.2−5.6 μm showed a very high DRH value (>81%). In this particular case for the size range 3.2−5.6 μm, given the high DRH value, the particles are assumed to be a mixture of organic and inorganic compounds, with the organic fraction potentially being water-insoluble and having a negligible effect on the DRH due to its solubility limitations. However, for the size ranges 1.8−3.2 and 5.6−10 μm, the lowering of DRH compared to pure atmospheric inorganic salts is assumed to imply the mixing of water-soluble organic compounds with inorganic compounds.[46−48] For the size range 1.0−1.8 μm, we observed a reduction in Δf_N by >30% at RH = ~42% indicating a higher water uptake. Based on $d(\Delta f_N)/d(RH) \geq 1$ the DRH for 1.0−1.8 μm appeared to be ~45−53%, which is consistent with the highest κ_m (~0.44, see discussion below) among all the size ranges measured during this campaign.[6] The low DRH for this size range may imply that the organic−inorganic (sea salt) mixture consisted of organic material that was highly water-soluble. The assumptions about particle species in each size range rely on dominant species in the atmosphere, considering factors like particle size, hygroscopicity parameters, and the DRH of prominent chemical compounds such as NaCl, $NH_4(SO_4)_2$, etc.; however, the lack of chemical composition data during the sampling period limits precise determinations.

Figure 3 shows the size-resolved mass-based hygroscopic growth factors (gf_m) and the corresponding mass-based hygroscopicity parameters (κ_m) for the ambient aerosol particles calculated from the QCM measurements (methodology described in SI, Texts S4 and S5) as a function of the exposure of the ambient aerosol samples to a wide range of RH (2−90%). Figure 3a shows the increase in the growth factor resulting from the water uptake on exposure to humid air. The change in growth factor as a function of RH also varies with particle size range (as indicated by the different markers). For

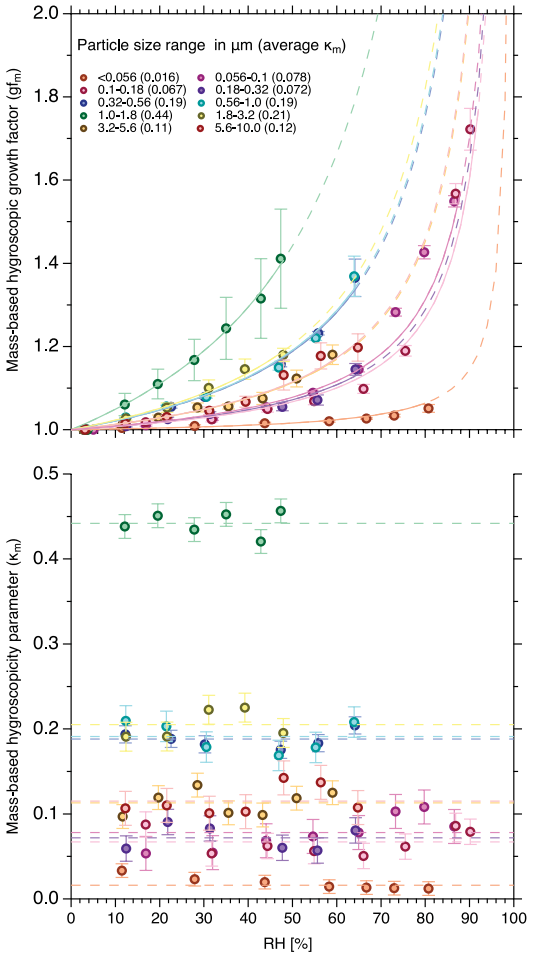

Figure 3. Size-resolved hygroscopicity measurements of ambient aerosol particles at the high-altitude site, Munnar, during the Monsoon season (August−September 2021). (a) Mass-based hygroscopic growth factor (gf_m) derived using a quartz crystal microbalance (QCM) for ten different size ranges of ambient aerosol particles at different relative humidity (RH) conditions in the subsaturated regime (circles). The solid lines represent the κ-Köhler growth factor fits obtained using the mean value of the mass-based hygroscopicity parameter (κ_m) while the dashed lines illustrate the corresponding values within the extrapolation range. The error bars represent the variations in gf_m averaged over the mass change corresponding to different overtone frequencies of the QCM sensor under respective RH conditions. The values in parentheses are the mean κ_m values corresponding to the respective size ranges. (b) The data points are the κ_m values calculated based on the gf_m (as shown in (a)) using the κ-Köhler theory for different RH conditions in the subsaturated regime. The dashed lines represent the mean κ_m value for each size range of ambient aerosol particles, and the error bars represent one standard deviation.

https://doi.org/10.1021/acsearthspacechem.3c00347
ACS Earth Space Chem. 2024, 8, 983−991

each size range, a maximum limit of RH was observed beyond which the estimation of gf_m was not possible due to QCM's inability to measure the actual mass of particles beyond deliquescence, as observed in other reports in the literature.[6] Accordingly, the highest gf_m = 1.72 was recorded at RH = 90% for the size range of 100−180 nm. The pronounced variations in gf_m between particles of different sizes for a given RH indicate the varying chemical composition and hygroscopicity across the sampled size ranges.

Figure 3b shows the size-dependent average κ_m values, calculated using the hygroscopic growth factors in Figure 3a. For each particle size range, the values of κ_m varied within a very small range (average $\kappa_m \pm 0.007$). Such a low variation of κ_m for a given size range measured over the wide range of RH may indicate the behavior of an ideal solution,[49] suggesting that hygroscopicity is dominated by nondissociating organic compounds, as hygroscopic inorganic components typically exhibit nonideal mixing with water. The average κ_m, as indicated by the dashed lines in Figure 3b for different size ranges, varied significantly between 0.016 (<0.056 nm) and 0.44 (1.0−1.8 μm) over the investigated RH range. This implies that κ_m is a function of size, and it is likely that each size fraction corresponds to a different chemical composition. For example, the small increase in κ_m from 0.016 to 0.078 for particles <56 nm to particles 56−100 nm, respectively, is potentially owing to aging processes.[50] Aerosol particles in the size ranges <180 nm exhibited very low average κ_m (0.05), which may be primarily due to the strong dominance of organic compounds in these size ranges, further supported by the absence of DRH.[4,22,51] It may also be noted that if a substantial fraction of a particle is made up of crystalline solids that do not exhibit any water uptake and no response to changes in RH, the particle phase and structure can lead to lowering of κ_m[52] (0.07 for the size range 180−320 nm in our case). The particles in the size range of 320 nm−1 μm were moderately hygroscopic (average κ_m = 0.19), indicating the influence of inorganic salts.[53] The particle size range 1.0−1.8 μm exhibited highest κ_m (0.44), which implies the presence of highly hygroscopic material such as sea salt[54] mixed with organic compounds. Even larger particles showed a decrease in corresponding κ_m, which may be attributable to the presence of dust particles,[55] which are transported at this site during monsoon season.[42] The gf_m for each size range over the wide range of RH values is very well explained by the fit obtained from κ-Köhler parametrization.[38]

Figure 4 shows the size dependency of κ_m in the subsaturated regime measured by QCM together with κ_{CCN} (Text S2) in the supersaturated regime determined by size-resolved CCN measurements and aerosol size distributions obtained by SMPS and UV-APS. The submicrometer particles show a bimodal number size distribution with an Aitken mode peak at 63 nm and an accumulation mode at 145 nm, while the mass size distributions peak at 350 nm and 3 μm, respectively. The average κ_{CCN} increased from a value of 0.28 for the Aitken mode particles to 0.47 for the accumulation mode particles. In the submicrometer range, κ_m exhibited a nominal increase with particle size,[53] in parallel with the increase in κ_{CCN}, albeit at much lower absolute values. This increase likely reflects the decrease of organic fraction with size in the submicrometer range, which is supported by the appearance of deliquescence in the size range above 180 nm, indicating the presence of inorganic salts. In the supermicrometer range (for particles ≥1 μm), κ_m peaked due to the potential presence of NaCl particles

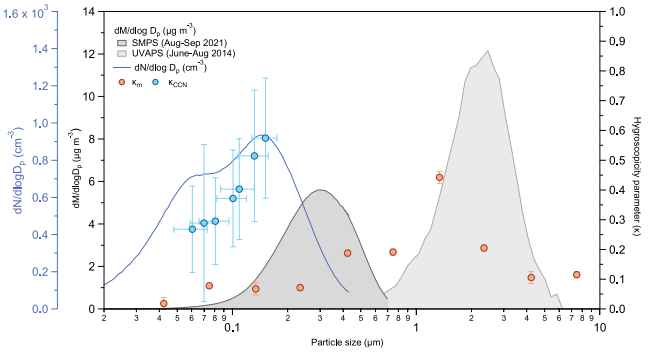

Figure 4. Aerosol size distributions, hygroscopicity parameters derived from quartz crystal microbalance (QCM) experiments (κ_m), and from size-resolved cloud condensation nuclei (CCN) measurements (κ_{CCN}). The number size distribution obtained using a scanning mobility particle sizer (SMPS) over the size range of 10−430 nm (blue curve) was measured during the sampling period and exhibited a bimodal distribution. The mass size distributions (dark gray shaded area) were derived based on the aerosol number size distribution by assuming a density of 1.2 g cm^{-3} for the submicrometer range. The mass size distribution for the supermicrometer range (light gray shaded area) was obtained using ultraviolet aerodynamic particle sizer (UV-APS) measurements during the same season (June−August) but for a different year (2014). The hygroscopic parameters derived from QCM experiments (κ_m; orange points) and size-resolved CCN measurements (κ_{CCN}; blue points) are shown for comparison. The error bars for κ_m and κ_{CCN} indicate the measurement uncertainty and variability, respectively.

in the size range 1.0−1.8 μm and decreased again in the higher size ranges (>1.8 μm) likely because of the presence of dust particles. The fact that the average value of κ_m (0.18) obtained from QCM measurements across all the sampled size ranges in the subsaturated regime was lower than the average κ_{CCN} (0.39) may be due to the solubility limitation[28,56−59] of organic and inorganic compounds in ambient aerosol particles below the DRH. Most inorganic species are completely dissolved beyond the DRH point in the subsaturated regime and therefore the κ_{CCN} is obtained assuming complete solubility of particles.[38,60]

In contrast to the QCM measurements, the hygroscopicity parameters obtained in previous studies using the HTDMA technique (κ_{HTDMA}) are consistent with κ_{CCN} in most cases, as the particle hygroscopicity is determined based on the increase in the particle size during water uptake above the DRH point, and thus is not subject to solubility limitation.[60−62] Because of technical limitations, particularly the small changes in diameter corresponding to mass growth factors smaller than 2.0, the HTDMA technique cannot measure the changes in the hygroscopic properties of aerosols exposed to RH below the DRH point in the subsaturated regime.[63] In contrast, the QCM technique, which is not subject to these limitations, can be used to understand the water uptake characteristics of aerosol particles in the subsaturated regime below DRH and substantially enhance our understanding about solubility limitations of organic and inorganic compounds in the lower RH region. For example, the hygroscopic growth at low RH (typically <50%) significantly influences the physical properties of aerosol particles, including viscosity and phase morphology. Phase transitions occurring at lower RH values encompass various phenomena such as liquid−liquid phase separation, efflorescence, and the formation of highly viscous and semisolid amorphous states like glasses and gels.[64,65] Thus,

https://doi.org/10.1021/acsearthspacechem.3c00347
ACS Earth Space Chem. 2024, 8, 983−991

an enhancement in the knowledge about subsaturated water uptake characteristics is crucial for accurately quantifying the radiative forcing effects of ambient aerosol particles in the atmosphere.[39,66,67] The strong size dependence of κ_m also indicated varying chemical compositions for the different size ranges measured in this study.

4. SUMMARY AND ATMOSPHERIC IMPLICATIONS

We report the first results based on a high-sensitivity QCM technique to investigate the mass-based growth factor and hygroscopicity parameter of size−resolved ambient aerosols over a wide range of RH values from a relatively pristine high−altitude site in India. For the investigated size ranges, the pronounced variations in gf_m below the DRH provided an opportunity to better understand the changes in ambient aerosol properties even at low RH values, which may not be revealed by size-based growth factor measurements.[45,63] These measurements clearly highlight the important and critical role in knowing the changes in aerosol properties based on their RH history for an improved understanding of water uptake, phase transition, and radiative impact of atmospheric aerosol particles.[25] Based on the estimated κ_m values, the ambient aerosol particles exhibited the behavior of an ideal solution[60] and strong size-dependent chemical composition. We further observed a pronounced size dependency of the DRH values potentially resulting from complexities of organic solubility in organic−inorganic mixtures.[22] Such a complexity owing to the presence of various organic species may alter the hygroscopic behavior of atmospheric aerosol particles due to phase transitions and changes in physical properties. The understanding of CCN activation in the supersaturated regime under the assumption of complete solubility of particles is relatively well established. However, the understanding of the thermodynamic properties associated with particle growth in the subsaturated regime still remains a challenge. Our findings emphasize the need for additional experiments on ambient and atmospherically relevant laboratory-generated aerosol particles using high-sensitivity techniques such as QCM. We demonstrated the importance of this technique to better understand the sudden changes in aerosol properties resulting from exposure to a wide range of atmospheric RH conditions. The enhancement in our understanding of the complex interplay between water vapor and aerosol particles will help in developing more accurate models to effectively describe the role of aerosols in atmospheric processes to reduce climate uncertainties and assess the impact of air pollution on human and ecosystem health.

■ ASSOCIATED CONTENT

Supporting Information

The Supporting Information is available free of charge at https://pubs.acs.org/doi/10.1021/acsearthspacechem.3c00347.

Additional experimental details, validation of the proposed method, calculation and estimation of the various parameters, materials, and detailed methodology, and results of the additional data analysis (PDF)

■ AUTHOR INFORMATION

Corresponding Authors

Christi Jose − *Environemntal Engineering Division, Dept of Civil Engineering and Centre for Atmospheric and Climate Sciences, Indian Institute of Technology Madras, Chennai 600036, India*; Email: christijose@cacs.iitm.ac.in

Pengfei Liu − *School of Earth and Atmospheric Sciences, Georgia Institute of Technology, Atlanta, Georgia 30332, United States*; Email: pengfei.liu@eas.gatech.edu

Sachin S. Gunthe − *Environemntal Engineering Division, Dept of Civil Engineering and Centre for Atmospheric and Climate Sciences, Indian Institute of Technology Madras, Chennai 600036, India*; orcid.org/0000-0002-7903-7783; Email: s.gunthe@iitm.ac.in

Authors

Aishwarya Singh − *Environemntal Engineering Division, Dept of Civil Engineering and Centre for Atmospheric and Climate Sciences, Indian Institute of Technology Madras, Chennai 600036, India*

Kavyashree N. Kalkura − *Environemntal Engineering Division, Dept of Civil Engineering and Centre for Atmospheric and Climate Sciences, Indian Institute of Technology Madras, Chennai 600036, India*

George V. Jose − *Dept of Civil Engineering, Indian Institute of Technology Bombay, Mumbai 400076, India*

Shailina Srivastava − *Environemntal Engineering Division, Dept of Civil Engineering and Centre for Atmospheric and Climate Sciences, Indian Institute of Technology Madras, Chennai 600036, India*

Rameshchand K. Ammini − *Dept of Mechanical Engineering, College of Engineering Munnar, Munnar 685612, India*

Shweta Yadav − *Dept of Environmental Sciences, Central University of Jammu, Samba 181143, India*

Raghunathan Ravikrishna − *Centre for Atmospheric and Climate Sciences and Dept of Chemical Engineering, Indian Institute of Technology Madras, Chennai 600036, India*

Meinrat O. Andreae − *Max Planck Institute for Chemistry, Mainz 55128, Germany; Scripps Institution of Oceanography, University of California San Diego, La Jolla, California 92093, United States; Department of Geology and Geophysics, King Saud University, Riyadh 11451, Saudi Arabia*

Scot T. Martin − *Department of Earth and Planetary Sciences and John A. Paulson School of Engineering & Applied Sciences, Harvard University, Cambridge, Massachusetts 02138, United States*; orcid.org/0000-0002-8996-7554

Complete contact information is available at: https://pubs.acs.org/10.1021/acsearthspacechem.3c00347

Author Contributions

S.S.G. conceived the idea. S.S.G. and P.L. conceptualized the study and designed the research. C.J. further developed and validated the QCM measurements for the ambient aerosol studies. C.J. performed the field measurement campaign to collect the aerosol samples with support from A.S., K.N.K., and R.K.A. C.J. performed all the laboratory experiments using QCM with support from S.S. G.V.J. performed the satellite data analysis to obtain the AOD values. C.J. carried out the data analysis obtained from QCM with input from P.L. and S.S.G. C.J. and A.S. performed the scientific interpretation of the QCM data under the mentorship of R.R., S.S.G., and P.L. C.J. wrote the first draft of manuscript under the mentorship of S.S.G. with inputs from P.L. and R.R. and further edits from S.Y. M.O.A and S.T.M. further provided critical and valuable inputs on the manuscript.

Notes

The authors declare no competing financial interest.

■ ACKNOWLEDGMENTS

S.S.G. gratefully acknowledges funding from the Ministry of Earth Sciences (MoES; sanction number MoES/16/20/12-RDEAS dated 31. Mar.2014), Government of India, for the purchase of the Cloud Condensation Nuclei Counter (CCNc). This work was supported by partial funding from the Ministry of Earth Sciences (MoES; sanction number MoES/16/04/2017-APHH (PROMOTE)), the Government of India, and the Department of Science and Technology (sanction number DST/CCP/CoE/141/2018C), the Government of India for the purchase of Quartz Crystal Microbalance (QCM). P.L. acknowledges the start-up funding support from the Georgia Institute of Technology. C.J. acknowledges the Department of Science and Technology, the Government of India for the fellowship. S.S.G. gratefully acknowledge the partial financial support from Sharp Business Systems (India) Private Limited for establishing the NABHA Laboratory. The authors acknowledge the valuable support and help provided by the staff at the College of Engineering Munnar during the campaign, with special and critical help from Jyothish Jose. C.J. acknowledges the invaluable assistance provided by Emil Varghese during the laboratory experiments. We are thankful to the support staff from Biolin Scientific, and Specialise Instruments Marketing Company, Mumbai, India, for their help during the experiments. We acknowledge the National Aeronautics and Space Administration (NASA) for making Moderate Resolution Imaging Spectroradiometer (MODIS) Earth data available to the user community.

■ REFERENCES

(1) Cheung, H. H. Y.; Yeung, M. C.; Li, Y. J.; Lee, B. P.; Chan, C. K. Relative Humidity-Dependent HTDMA Measurements of Ambient Aerosols at the HKUST Supersite in Hong Kong, China. *Aerosol Sci. Technol.* **2015**, *49* (8), 643−654.

(2) Liu, Y.; Laskin, A. Hygroscopic Properties of CH3SO3Na, CH3SO3NH4, (CH3SO3)2Mg, and (CH3SO3)2Ca Particles Studied by Micro-FTIR Spectroscopy. *J. Phys. Chem. A* **2009**, 1531−1538, DOI: 10.1021/jp8079149.

(3) Liu, Y.; Yang, Z.; Desyaterik, Y.; Gassman, P. L.; Wang, H.; Laskin, A. Hygroscopic Behavior of Substrate-Deposited Particles Studied by Micro-FT-IR Spectroscopy and Complementary Methods of Particle Analysis (Analytical Chemistry (2008) 80, (633−642)). *Anal. Chem.* **2008**, *80* (18), 7179.

(4) Demou, E.; Visram, H.; Donaldson, D. J.; Makar, P. A. Uptake of Water by Organic Films: The Dependence on the Film Oxidation State. *Atmos. Environ.* **2003**, *37* (25), 3529−3537.

(5) Liu, P.; Li, Y. J.; Wang, Y.; Gilles, M. K.; Zaveri, R. A.; Bertram, A. K.; Martin, S. T. Lability of Secondary Organic Particulate Matter. *Proc. Natl. Acad. Sci. U. S. A.* **2016**, *113* (45), 12643−12648.

(6) Chao, H. J.; Huang, W. C.; Chen, C. L.; Chou, C. C. K.; Hung, H. M. Water Adsorption vs Phase Transition of Aerosols Monitored by a Quartz Crystal Microbalance. *ACS Omega* **2020**, *5* (49), 31858−31866.

(7) Liu, P.; Song, M.; Zhao, T.; Gunthe, S. S.; Ham, S.; He, Y.; Qin, Y. M.; Gong, Z.; Amorim, J. C.; Bertram, A. K.; Martin, S. T. Resolving the Mechanisms of Hygroscopic Growth and Cloud Condensation Nuclei Activity for Organic Particulate Matter. *Nat. Commun.* **2018**, *9* (1), 4076 DOI: 10.1038/s41467-018-06622-2.

(8) Liu, Y. J.; Zhu, T.; Zhao, D. F.; Zhang, Z. F. Investigation of the Hygroscopic Properties of Ca(NO3) 2 and Internally Mixed Ca(NO3)2/CaCO 3 Particles by Micro-Raman Spectrometry. *Atmos Chem. Phys.* **2008**, *8* (23), 7205−7215.

(9) Ling, T. Y.; Chan, C. K. Partial Crystallization and Deliquescence of Particles Containing Ammonium Sulfate and Dicarboxylic Acids. *J. Geophys. Res.: Atmos.* **2008**, *113* (14), D14205 DOI: 10.1029/2008JD009779.

(10) Pope, F. D.; Dennis-smither, B. J.; Griffiths, P. T.; Clegg, S. L.; Cox, R. A. Studies of Single Aerosol Particles Containing Malonic Acid, Glutaric Acid, and Their Mixtures with Sodium Chloride. I. Hygroscopic Growth. *Growth Factors* **2010**, *114*, 5335−5341.

(11) Choi, M. Y.; Chan, C. K. The Effects of Organic Species on the Hygroscopic Behaviors of Inorganic Aerosols. *Environ. Sci. Technol.* **2002**, *36* (11), 2422−2428.

(12) Peng, C.; Chan, C. K. The Water Cycles of Water-Soluble Organic Salts of Atmospheric Importance. *Atmos. Environ.* **2001**, *35* (7), 1183−1192.

(13) Ahn, K. H.; Kim, S. M.; Jung, H. J.; Lee, M. J.; Eom, H. J.; Maskey, S.; Ro, C. U. Combined Use of Optical and Electron Microscopic Techniques for the Measurement of Hygroscopic Property, Chemical Composition, and Morphology of Individual Aerosol Particles. *Anal. Chem.* **2010**, *82* (19), 7999−8009.

(14) Eom, H. J.; Gupta, D.; Li, X.; Jung, H. J.; Kim, H.; Ro, C. U. Influence of Collecting Substrates on the Characterization of Hygroscopic Properties of Inorganic Aerosol Particles. *Anal. Chem.* **2014**, *86* (5), 2648−2656.

(15) Gupta, D.; Kim, H.; Park, G.; Li, X.; Eom, H. J.; Ro, C. U. Hygroscopic Properties of NaCl and NaNO3Mixture Particles as Reacted Inorganic Sea-Salt Aerosol Surrogates. *Atmos Chem. Phys.* **2015**, *15* (6), 3379−3393.

(16) Prenni, A. J.; Petters, M. D.; Kreidenweis, S. M.; DeMott, P. J.; Ziemann, P. J. Cloud Droplet Activation of Secondary Organic Aerosol. *J. Geophys. Res. Atmos.* **2007**, *112* (10), D10223 DOI: 10.1029/2006JD007963.

(17) Zieger, P.; Väisänen, O.; Corbin, J. C.; Partridge, D. G.; Bastelberger, S.; Mousavi-Fard, M.; Rosati, B.; Gysel, M.; Krieger, U. K.; Leck, C.; Nenes, A.; Riipinen, I.; Virtanen, A.; Salter, M. E. Revising the Hygroscopicity of Inorganic Sea Salt Particles. *Nat. Commun.* **2017**, *8*, 15883 DOI: 10.1038/ncomms15883.

(18) Rose, D.; Gunthe, S. S.; Mikhailov, E.; Frank, G. P.; Dusek, U.; Andreae, M. O.; Pöschl, U. Calibration and Measurement Uncertainties of a Continuous-Flow Cloud Condensation Nuclei Counter (DMT-CCNC): CCN Activation of Ammonium Sulfate and Sodium Chloride Aerosol Particles in Theory and Experiment. *Atmos Chem. Phys.* **2008**, *8* (5), 1153−1179.

(19) Petters, M. D.; Prenni, A. J.; Kreidenweis, S. M.; DeMott, P. J. On Measuring the Critical Diameter of Cloud Condensation Nuclei Using Mobility Selected Aerosol. *Aerosol Sci. Technol.* **2007**, *41* (10), 907−913.

(20) Pöhlker, M. L.; Pöhlker, C.; Ditas, F.; Klimach, T.; De Angelis, I. H.; Araújo, A.; Brito, J.; Carbone, S.; Cheng, Y.; Chi, X.; Ditz, R.; Gunthe, S. S.; Kesselmeier, J.; Könemann, T.; Lavrič, J. V.; Martin, S. T.; Mikhailov, E.; Moran-Zuloaga, D.; Rose, D.; Saturno, J.; Su, H.; Thalman, R.; Walter, D.; Wang, J.; Wolff, S.; Barbosa, H. M. J.; Artaxo, P.; Andreae, M. O.; Pöschl, U. Long-Term Observations of Cloud Condensation Nuclei in the Amazon Rain Forest - Part 1: Aerosol Size Distribution, Hygroscopicity, and New Model Parametrizations for CCN Prediction. *Atmos Chem. Phys.* **2016**, *16* (24), 15709−15740.

(21) Tang, M.; Chan, C. K.; Li, Y. J.; Su, H.; Ma, Q.; Wu, Z.; Zhang, G.; Wang, Z.; Ge, M.; Hu, M.; He, H.; Wang, X. A Review of Experimental Techniques for Aerosol Hygroscopicity Studies. *Atmos Chem. Phys.* **2019**, *19* (19), 12631−12686.

(22) Li, W.; Teng, X.; Chen, X.; Liu, L.; Xu, L.; Zhang, J.; Wang, Y.; Zhang, Y.; Shi, Z. Organic Coating Reduces Hygroscopic Growth of Phase-Separated Aerosol Particles. *Environ. Sci. Technol.* **2021**, *55* (24), 16339−16346.

(23) Liu, P.; Song, M.; Zhao, T.; Gunthe, S. S.; Ham, S.; He, Y.; Qin, Y. M.; Gong, Z.; Amorim, J. C.; Bertram, A. K.; Martin, S. T. Resolving the Mechanisms of Hygroscopic Growth and Cloud Condensation Nuclei Activity for Organic Particulate Matter. *Nat. Commun.* **2018**, *9*, 4076 DOI: 10.1038/s41467-018-06622-2.

(24) Liu, P.; Li, Y. J.; Wang, Y.; Gilles, M. K.; Zaveri, R. A.; Bertram, A. K.; Martin, S. T. Lability of Secondary Organic Particulate Matter. *Proc. Natl. Acad. Sci. U. S. A.* **2016**, *113* (45), 12643−12648.
(25) Zhao, P.; Ge, S.; Su, J.; Ding, J.; Kuang, Y. Relative Humidity Dependence of Hygroscopicity Parameter of Ambient Aerosols. *Journal of Geophysical Research: Atmospheres* **2022**, *127* (8), 1−10.
(26) Liu, P.; Li, Y. J.; Wang, Y.; Bateman, A. P.; Zhang, Y.; Gong, Z.; Bertram, A. K.; Martin, S. T. Highly Viscous States Affect the Browning of Atmospheric Organic Particulate Matter. *ACS Cent Sci.* **2018**, *4* (2), 207−215.
(27) Gupta, P.; Banerjee, A.; Gupta, N. J. Spatio-Temporal Study on Changing Trend of Land Use and Land Cover Pattern in Munnar Area, Idukki District, Western Ghats, India. *Indian J. Geo-Mar. Sci.* **2020**, *49* (06), 1055−1067.
(28) Rastak, N.; Pajunoja, A.; Acosta Navarro, J. C.; Ma, J.; Song, M.; Partridge, D. G.; Kirkevåg, A.; Leong, Y.; Hu, W. W.; Taylor, N. F.; Lambe, A.; Cerully, K.; Bougiatioti, A.; Liu, P.; Krejci, R.; Petäjä, T.; Percival, C.; Davidovits, P.; Worsnop, D. R.; Ekman, A. M. L.; Nenes, A.; Martin, S.; Jimenez, J. L.; Collins, D. R.; Topping, D. O.; Bertram, A. K.; Zuend, A.; Virtanen, A.; Riipinen, I. Microphysical Explanation of the RH-Dependent Water Affinity of Biogenic Organic Aerosol and Its Importance for Climate. *Geophys. Res. Lett.* **2017**, *44* (10), 5167−5177.
(29) Marple, V. A.; Rubow, K. L.; Behm, S. M. A Microorifice Uniform Deposit Impactor (Moudi): Description, Calibration, and Use. *Aerosol Sci. Technol.* **1991**, *14* (4), 434−436.
(30) Marple, V.; Olson, B.; Romay, F.; Hudak, G.; Geerts, S. M.; Lundgren, D. Second Generation Micro-Orifice Uniform Deposit Impactor, 120 MOUDI-II: Design, Evaluation, and Application to Long-Term Ambient Sampling. *Aerosol Sci. Technol.* **2014**, *48* (4), 427−433.
(31) Reviakine, I.; Johannsmann, D.; Richter, R. P. Hearing What You Cannot See and Visualizing What You Hear: Interpreting Quartz Crystal Microbalance Data from Solvated Interfaces. *Anal. Chem.* **2011**, *83* (23), 8838−8848.
(32) Zobrist, B.; Soonsin, V.; Luo, B. P.; Krieger, U. K.; Marcolli, C.; Peter, T.; Koop, T. Ultra-Slow Water Diffusion in Aqueous Sucrose Glasses. *Phys. Chem. Chem. Phys.* **2011**, *13* (8), 3514−3526.
(33) Starzak, M.; Peacock, S. D. Water Activity Coefficient in Aqueous Solutions of Sucrose -a Comprehensive Data Analysis. *Zuckerindustrie* **1997**, *122* (5), 380−387.
(34) Norrish, R. Equation for the Activity Coefficients and Equilibrium Relative Humidities. *JInternational Journal of Food Science & Technology* **1966**, *1*, 25−39.
(35) Arenas, K. J. L.; Schill, S. R.; Malla, A.; Hudson, P. K. Deliquescence Phase Transition Measurements by Quartz Crystal Microbalance Frequency Shifts. *J. Phys. Chem. A* **2012**, *116* (29), 7658−7667.
(36) Peng, C.; Chen, L.; Tang, M. A Database for Deliquescence and Efflorescence Relative Humidities of Compounds with Atmospheric Relevance. *Fundamental Research* **2022**, *2* (4), 578−587.
(37) Martin, S. T. Phase Transitions of Aqueous Atmospheric Particles. *Chem. Rev.* **2000**, *100* (9), 3403−3453.
(38) Petters, M. D.; Kreidenweis, S. M. A Single Parameter Representation of Hygroscopic Growth and Cloud Condensation Nucleus Activity. *Atmos Chem. Phys.* **2007**, *7* (8), 1961−1971.
(39) Zhao, P.; Ge, S.; Su, J.; Ding, J.; Kuang, Y. Relative Humidity Dependence of Hygroscopicity Parameter of Ambient Aerosols. *Journal of Geophysical Research: Atmospheres* **2022**, *127* (8), 1−10.
(40) Bian, Y. X.; Zhao, C. S.; Ma, N.; Chen, J.; Xu, W. Y. A Study of Aerosol Liquid Water Content Based on Hygroscopicity Measurements at High Relative Humidity in the North China Plain. *Atmos Chem. Phys.* **2014**, *14* (12), 6417−6426.
(41) DeCarlo, P. F.; Slowik, J. G.; Worsnop, D. R.; Davidovits, P.; Jimenez, J. L. Particle Morphology and Density Characterization by Combined Mobility and Aerodynamic Diameter Measurements. Part 1: Theory. *Aerosol Sci. Technol.* **2004**, *38* (12), 1185−1205.
(42) Valsan, A. E.; Ravikrishna, R.; Biju, C. V.; Pöhlker, C.; Després, V. R.; Huffman, J. A.; Pöschl, U.; Gunthe, S. S. Fluorescent Biological Aerosol Particle Measurements at a Tropical High-Altitude Site in Southern India during the Southwest Monsoon Season. *Atmos Chem. Phys.* **2016**, *16* (15), 9805−9830.
(43) Arenas, K. J. L.; Schill, S. R.; Malla, A.; Hudson, P. K. Deliquescence Phase Transition Measurements by Quartz Crystal Microbalance Frequency Shifts. *J. Phys. Chem. A* **2012**, *116* (29), 7658−7667.
(44) Brooks, S. D.; Wise, M. E.; Cushing, M.; Tolbert, M. A. Deliquescence Behavior of Organic/Ammonium Sulfate Aerosol. *Geophys. Res. Lett.* **2002**, *29* (19), 23-1 DOI: 10.1029/2002GL014733.
(45) Hu, D.; Qiao, L.; Chen, J.; Ye, X.; Yang, X.; Cheng, T.; Fang, W. Hygroscopicity of Inorganic Aerosols: Size and Relative Humidity Effects on the Growth Factor. *Aerosol Air Qual Res.* **2010**, *10* (3), 255−264.
(46) Smith, M. L.; You, Y.; Kuwata, M.; Bertram, A. K.; Martin, S. T. Phase Transitions and Phase Miscibility of Mixed Particles of Ammonium Sulfate, Toluene-Derived Secondary Organic Material, and Water. *J. Phys. Chem. A* **2013**, *117* (36), 8895−8906.
(47) Smith, M. L.; Kuwata, M.; Martin, S. T. Secondary Organic Material Produced by the Dark Ozonolysis Of-Pinene Minimally Affects the Deliquescence and Efflorescence of Ammonium Sulfate. *Aerosol Sci. Technol.* **2011**, *45* (2), 244−261.
(48) Smith, M. L.; Bertram, A. K.; Martin, S. T. Deliquescence, Efflorescence, and Phase Miscibility of Mixed Particles of Ammonium Sulfate and Isoprene-Derived Secondary Organic Material. *Atmos Chem. Phys.* **2012**, *12* (20), 9613−9628.
(49) Wang, Z.; Cheng, Y.; Ma, N.; Mikhailov, E.; Pöschl, U.; Su, H. Dependence of the Hygroscopicity Parameter κ on Particle Size, Humidity and Solute Concentration: Implications for Laboratory Experiments, Field Measurements and Model Studies. *Atmos. Chem. Phys. Discuss.* **2017**, 1−33.
(50) Zhang, S.; Shen, X.; Sun, J.; Zhang, Y.; Zhang, X.; Xia, C.; Hu, X.; Zhong, J.; Wang, J.; Liu, S. Atmospheric Particle Hygroscopicity and the Influence by Oxidation State of Organic Aerosols in Urban Beijing. *J. Environ. Sci. (China)* **2023**, *124*, 544−556.
(51) Shi, J.; Hong, J.; Ma, N.; Luo, Q.; He, Y.; Xu, H.; Tan, H.; Wang, Q.; Tao, J.; Zhou, Y.; Han, S.; Peng, L.; Xie, L.; Zhou, G.; Xu, W.; Sun, Y.; Cheng, Y.; Su, H. Measurement Report: On the Difference in Aerosol Hygroscopicity between High and Low Relative Humidity Conditions in the North China Plain. *Atmos Chem. Phys.* **2022**, *22* (7), 4599−4613.
(52) Petters, M. D.; Kreidenweis, S. M. A Single Parameter Representation of Hygroscopic Growth and Cloud Condensation Nucleus Activity - Part 2: Including Solubility. *Atmos Chem. Phys.* **2008**, *8* (20), 6273−6279.
(53) Wu, Z. J.; Zheng, J.; Shang, D. J.; Du, Z. F.; Wu, Y. S.; Zeng, L. M.; Wiedensohler, A.; Hu, M. Particle Hygroscopicity and Its Link to Chemical Composition in the Urban Atmosphere of Beijing, China, during Summertime. *Atmos Chem. Phys.* **2016**, *16* (2), 1123−1138.
(54) Zieger, P.; Väisänen, O.; Corbin, J. C.; Partridge, D. G.; Bastelberger, S.; Mousavi-Fard, M.; Rosati, B.; Gysel, M.; Krieger, U. K.; Leck, C.; Nenes, A.; Riipinen, I.; Virtanen, A.; Salter, M. E. Revising the Hygroscopicity of Inorganic Sea Salt Particles. *Nat. Commun.* **2017**, *8*, 15883 DOI: 10.1038/ncomms15883.
(55) Koehler, K. A.; Kreidenweis, S. M.; DeMott, P. J.; Petters, M. D.; Prenni, A. J.; Carrico, C. M. Hygroscopicity and Cloud Droplet Activation of Mineral Dust Aerosol. *Geophys. Res. Lett.* **2009**, *36* (8), 1−5.
(56) Riipinen, I.; Rastak, N.; Pandis, S. N. Connecting the Solubility and CCN Activation of Complex Organic Aerosols: A Theoretical Study Using Solubility Distributions. *Atmos Chem. Phys.* **2015**, *15* (11), 6305−6322.
(57) Dusek, U.; Frank, G. P.; Massling, A.; Zeromskiene, K.; Iinuma, Y.; Schmid, O.; Helas, G.; Hennig, T.; Wiedensohler, A.; Andreae, M. O. Water Uptake by Biomass Burning Aerosol at Sub-and Supersaturated Conditions: Closure Studies and Implications for the Role of Organics. *Atmos Chem. Phys.* **2011**, *11* (18), 9519−9532.

(58) Hersey, S. P.; Craven, J. S.; Metcalf, A. R.; Lin, J.; Lathem, T.; Suski, K. J.; Cahill, J. F.; Duong, H. T.; Sorooshian, A.; Jonsson, H. H.; Shiraiwa, M.; Zuend, A.; Nenes, A.; Prather, K. A.; Flagan, R. C.; Seinfeld, J. H. Composition and Hygroscopicity of the Los Angeles Aerosol: CalNex. *Journal of Geophysical Research Atmospheres* **2013**, *118* (7), 3016−3036.
(59) Wittbom, C.; Eriksson, A. C.; Rissler, J.; Roldin, P.; Nordin, E. Z.; Sjogren, S.; Nilsson, P. T.; Swietlicki, E.; Pagels, J.; Svenningsson, B. Effect of Solubility Limitation on Hygroscopic Growth and Cloud Drop Activation of SOA Particles Produced from Traffic Exhausts. *J. Atmos Chem.* **2018**, *75* (4), 359−383.
(60) Pajunoja, A.; Lambe, A. T.; Hakala, J.; Rastak, N.; Cummings, M. J.; Brogan, J. F.; Hao, L.; Paramonov, M.; Hong, J.; Prisle, N. L.; Malila, J.; Romakkaniemi, S.; Lehtinen, K. E. J.; Laaksonen, A.; Kulmala, M.; Massoli, P.; Onasch, T. B.; Donahue, N. M.; Riipinen, I.; Davidovits, P.; Worsnop, D. R.; Petäjä, T.; Virtanen, A. Adsorptive Uptake of Water by Semisolid Secondary Organic Aerosols. *Geophys. Res. Lett.* **2015**, *42* (8), 3063−3068.
(61) Wang, Y.; Li, Z.; Zhang, Y.; Du, W.; Zhang, F.; Tan, H.; Xu, H.; Fan, T.; Jin, X.; Fan, X.; Dong, Z.; Wang, Q.; Sun, Y. Characterization of Aerosol Hygroscopicity, Mixing State, and CCN Activity at a Suburban Site in the Central North China Plain. *Atmos Chem. Phys.* **2018**, *18* (16), 11739−11752.
(62) Wu, Z. J.; Poulain, L.; Henning, S.; Dieckmann, K.; Birmili, W.; Merkel, M.; Van Pinxteren, D.; Spindler, G.; Müller, K.; Stratmann, F.; Herrmann, H.; Wiedensohler, A. Relating Particle Hygroscopicity and CCN Activity to Chemical Composition during the HCCT-2010 Field Campaign. *Atmos Chem. Phys.* **2013**, *13* (16), 7983−7996.
(63) Laskina, O.; Morris, H. S.; Grandquist, J. R.; Qin, Z.; Stone, E. A.; Tivanski, A. V.; Grassian, V. H. Size Matters in the Water Uptake and Hygroscopic Growth of Atmospherically Relevant Multi-component Aerosol Particles. *J. Phys. Chem. A* **2015**, *119* (19), 4489−4497.
(64) Sheldon, C. S.; Choczynski, J. M.; Morton, K.; Diaz, T. P.; Davis, R. D.; Davies, J. F. Exploring the Hygroscopicity, Water Diffusivity, and Viscosity of Organic-Inorganic Aerosols - a Case Study on Internally-Mixed Citric Acid and Ammonium Sulfate Particles. *Environ. Sci.: Atmos.* **2023**, *3*, 24.
(65) Madawala, C. K.; Lee, H. D.; Kaluarachchi, C. P.; Tivanski, A. V. Probing the Water Uptake and Phase State of Individual Sucrose Nanoparticles Using Atomic Force Microscopy. *ACS Earth Space Chem.* **2021**, *5* (10), 2612−2620.
(66) Parsons, M. T.; Knopf, D. A.; Bertram, A. K. Deliquescence and Crystallization of Ammonium Sulfate Particles Internally Mixed with Water-Soluble Organic Compounds. *J. Phys. Chem. A* **2004**, *108* (52), 11600−11608.
(67) Wang, W.; Lei, T.; Zuend, A.; Su, H.; Cheng, Y.; Shi, Y.; Ge, M.; Liu, M. Effect of Mixing Structure on the Water Uptake of Mixtures of Ammonium Sulfate and Phthalic Acid Particles. *Atmos Chem. Phys.* **2021**, *21* (3), 2179−2190.

https://doi.org/10.1021/acsearthspacechem.3c00347
ACS Earth Space Chem. 2024, 8, 983−991